New Paleomagnetic and Stable-Isotope Results from the Nanxiong Basin, China: Implications for the K/T Boundary and the Timing of Paleocene Mammalian Turnover

William C. Clyde, Suyin Ting,[1] Kathryn E. Snell,[2] Gabriel J. Bowen,[3] Yongsheng Tong,[4] Paul L. Koch,[2] Qian Li,[4] and Yuanqing Wang[4]

Department of Earth Sciences, University of New Hampshire, James Hall, 56 College Road, Durham, New Hampshire 03824, U.S.A.
(e-mail: will.clyde@unh.edu)

ABSTRACT

The Nanxiong Basin (Guangdong Province, China) preserves the most complete Asian stratigraphic record of the Cretaceous-Paleogene (K/Pg) boundary extinction and the subsequent Paleocene mammalian radiation. Despite extensive study, the precise placement of the K/Pg boundary in the Nanxiong Basin sequence has been controversial, and the timing of subsequent mammalian turnover is poorly constrained. We present new paleomagnetic and geochemical data from the Late Cretaceous Pingling Formation (Nanxiong Group) and the overlying Paleocene Shanghu, Nongshan, and Guchengcun formations (Luofozhai Group). Our samples are directly correlated with previous geochemical and paleontological sampling localities, allowing for easy comparison with other local proxy records. Results indicate that the traditional placement of the K/Pg boundary at the base of a chaotic channel sandstone bed marking the highest stratigraphic appearance of dinosaur eggshell fragments and lowest stratigraphic appearance of Paleocene mammalian fossils lies about two-thirds of the way up Chron C29R, consistent with the placement of the boundary in all other well-documented sections. The average carbon isotope composition of paleosol carbonates decreases by >2‰ in the Early Paleocene, consistent with a major disruption to global carbon cycling after the K/Pg boundary. Constraints on the age of the first major Cenozoic mammalian turnover event in Asia (the Shanghuan-Nongshanian Asian Land Mammal Age boundary) support its placement near the top of Chron C27N, which coincides with a similar turnover in North America and geochemical changes recorded in several deep sea cores.

Online enhancements: appendix figure and tables.

Introduction

The Nanxiong Basin is an elongate extensional basin on the South China tectonic block that formed in the back arc of the Kula-Pacific subduction zone during the late Mesozoic (fig. 1). It preserves an ~5000-m-thick section of Cretaceous to Paleogene fossiliferous red beds of fluvial and lacustrine origin, much of which is well exposed. The basin contains the most continuous record currently known in Asia of the K/Pg boundary interval and the subsequent Early Paleocene mammalian radiation. The precise placement of the K/Pg boundary in the Nanxiong Basin sequence has been the subject of considerable controversy, with important implications for the rate and global synchroneity of extinction. Its location on the other side of the Earth from the putative K/Pg impact site makes it particularly important for understanding the far-field effects of the impact on a continental system. The Paleocene Shanghuan and Nongshanian Asian Land Mammal Ages (ALMAs) are also well documented in the Nanxiong Basin, providing an op-

Manuscript received June 5, 2009; accepted November 9, 2009.

[1] Museum of Natural Science, Louisiana State University, Baton Rouge, Louisiana 70803, U.S.A.

[2] Department of Earth and Planetary Sciences, University of California, Santa Cruz, California 95064, U.S.A.

[3] Department of Earth and Atmospheric Sciences, 550 Stadium Mall Drive, Purdue University, West Lafayette, Indiana 47907, U.S.A.

[4] Institute of Vertebrate Paleontology and Paleoanthropology, Chinese Academy of Sciences, P.O. Box 643, Beijing 100044, China.

[The Journal of Geology, 2010, volume 118, p. 131–143] © 2010 by The University of Chicago.
All rights reserved. 0022-1376/2010/11802-0002$15.00. DOI: 10.1086/649893

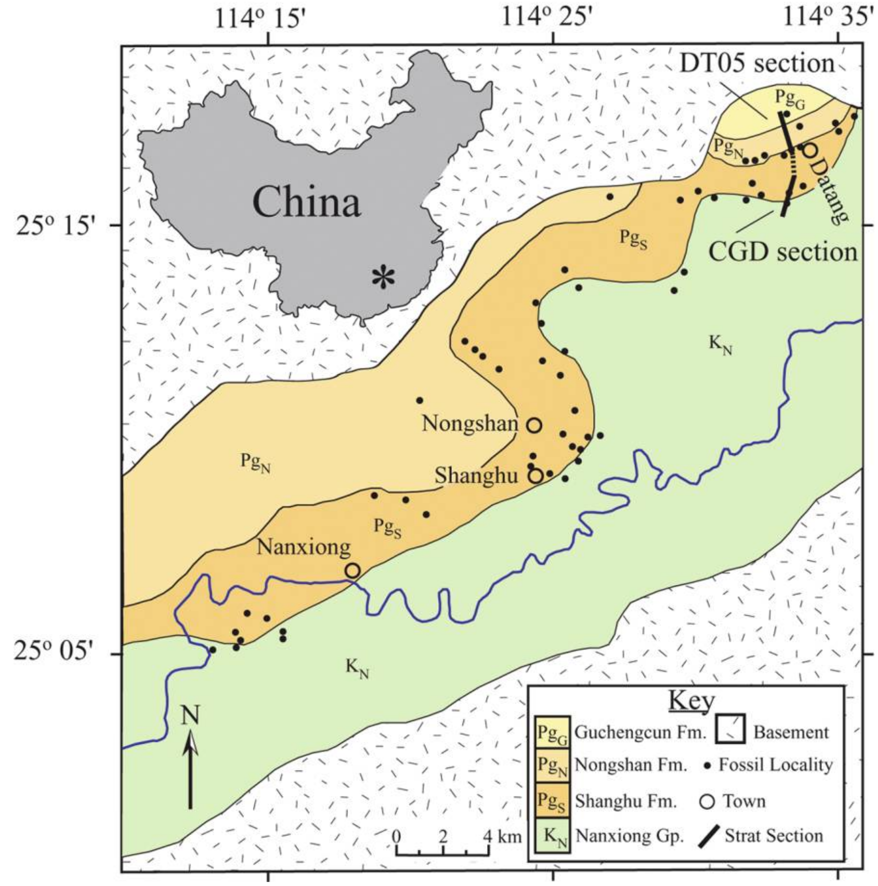

Figure 1. General geological map of Nanxiong Basin, adapted from Li and Ting (1983), showing vertebrate fossil localities, key geographic features, and the location of stratigraphic sections.

portunity to correlate these poorly known land mammal ages with the global timescale. We undertook magnetostratigraphic and chemostratigraphic analysis of a 1250-m section encompassing the latest Cretaceous Pingling Formation (Nanxiong Group) and the overlying Paleocene Shanghu, Nongshan, and Guchengcun formations (Luofozhai Group) in order to evaluate the different proposed placements for the K/Pg boundary and better constrain the timing of subsequent mammalian radiation and turnover in Asia.

Previous Research

Cretaceous-Paleogene Boundary. The exact placement of the Cretaceous-Paleogene boundary in the Nanxiong Basin has been the subject of controversy since it was first identified in the 1920s (see review by Taylor et al. [2006]). Globally, the boundary is defined by an iridium anomaly and coincident mass extinctions in marine and terrestrial biota, thought to have been caused by a large-meteorite impact (Molina et al. 2006). Despite this clearly defined boundary concept, the array of geochemical, geophysical, biostratigraphic, and sedimentological data from the Nanxiong Basin has led to conflicting interpretations of the exact placement of the boundary in this sequence. The different placements of the boundary imply different temporal patterns of extinction, so a resolution of this problem will help illustrate the response of Asian terrestrial ecosystems to the K/Pg boundary meteorite impact.

Much of the recent controversy in the placement of the Nanxiong K/Pg boundary began with the Chinese-German studies of the 1980s. Detailed fieldwork during that project resulted in extensive lithological, geochemical, paleomagnetic, and paleontological data, yet two different interpretations of the data emerged (Zhao et al. 1991; Erben et al. 1995; Stets et al. 1996). Zhao et al. (1991) argued for placing the boundary at the contact of the Pingling and Shanghu formations, which is marked by an irregular conglomeratic sandstone interval separating coarser-grained, lighter-colored red beds below from finer-grained, darker-colored red beds above. This interpretation (the "Zhao placement") is supported by the preservation of abundant dinosaur egg shell fragments, including some in situ nests, in the Pingling Formation and the preservation of Paleocene mammal fossils in the overlying Shanghu Formation (Hansen et al. 1994; Wang and Zhai 1995; Ting 1998; Wang et al. 1998). Stets et al. (1996), however, argued that the boundary should be placed at a position ~90 m below that of Zhao et al. (1991), where there are both a turnover in pollen assemblages and minor geochemical anomalies (Zhao et al. 1993, 2002). This interpretation (the "Stets placement") implies the survival of dinosaurs into the Paleogene and thus argues against a globally synchronized mass extinction coincident with an impact event. Later, Buck et al. (2004) accepted the Stets placement but argued that the dinosaur remains above that level were reworked because of debris flows in the upper Pingling Formation (their "Nanxiong Formation") and the lower Shanghu Formation. Taylor et al. (2006) reviewed the entire suite of evidence and concluded that the preponderance of evidence supports the Zhao placement.

Paleomagnetic data were collected through the key stratigraphic sections in the Nanxiong Basin by the Chinese-German field teams in the 1980s. Even though these data have had varied interpretations and have played an integral role in the various arguments for the positioning of the K/T boundary, they remain the only results of this type reported from the Nanxiong Basin and are poorly documented in the literature. For instance, Zhao et al. (1991) report the stratigraphic positions of three different normal-polarity zones in the Chinese-German Datang Section ("CGD section" of Erben et al. 1995) but do not provide any supporting evidence for them. Contrarily, Erben et al. (1995) and Stets et al. (1996) document only a single reversal in that section and do not mention the other reversals identified by Zhao et al. (1991), even though they are purportedly discussing results from the same underlying samples. In addition, Russell et al. (1993) argue for a different correlation of the magnetostratigraphy reported by Zhao et al. (1991) with the timescale. Finally, many of the original data on which the varying interpretations are based are not documented in detail, so it is difficult to evaluate their reliability and make an independent assessment of these different conclusions. Our renewed magnetostratigraphic sampling was designed to resolve these ongoing uncertainties.

Shanghuan-Nongshanian ALMA Boundary. In addition to its well-preserved K/Pg boundary interval, the Nanxiong Basin is well known for its Early Paleocene mammalian fossil record. The Nanxiong Basin represents the type area for both the Shanghuan and the Nongshanian ALMAs. Several very important fossils are known from here, including *Petrolemur brevirostre* (Tong 1979) and *Radinskya yupingae* (McKenna et al. 1989). *Petrolemur* is known from a single specimen and was originally interpreted as a Paleocene euprimate but was later attributed to other groups, including Ungulata (McKenna and Bell 1997). *Radinskya* is still thought to be closely related to perissodactyls, but its exact classification is uncertain (McKenna and Bell 1997). Although the phylogenetic positions of these taxa remain controversial, they represent potential candidates for Paleocene members of extant ("modern") orders that first appeared elsewhere at the Paleocene-Eocene boundary (Gingerich 2006). Despite the importance of the Nanxiong faunas for tracking the post-K/Pg boundary recovery of vertebrates in Asia and for understanding Holarctic biogeography, little stratigraphic work has been done to correlate them outside of Asia. The timely development of a coherent stratigraphic framework for these localities is also important because of the rapid agricultural and commercial development in the area. Of the 54 fossil localities documented from the Paleocene of the Nanxiong Basin, ~20 have been destroyed in recent years because of development. Many other localities are in imminent danger as housing developments spread into these areas at a fast rate.

Methods

We collected samples for paleomagnetic and isotopic analysis from two superimposed stratigraphic sections within the Pingling, Shanghu, Nongshan, and Guchengcun formations in the northeastern part of the Nanxiong Basin. The Late Cretaceous to Paleogene strata in the Nanxiong Basin are gently tilted (~20°) toward the north. The first and stratigraphically lowest section we sampled is the CGD section, which was logged by Erben et al. (1995) and used by several other studies (Zhao et al. 1991; Stets et al. 1996; Taylor et al. 2006). This section is 465 m thick, begins in the upper Pingling Formation, and ends in the Shanghu Formation. For purposes of discussion, we use the stratigraphic thickness and associated levels for the CGD section of Zhao et al. (1991) and Stets et al. (1996), which correct for a 16-m fault that was not accounted for in the original Erben et al. (1995) section; however, our data tables list both the original Erben et al. (1995) levels and the fault-adjusted levels. The second and stratigraphically higher section (the DT05 section) is 435 m thick, begins in the Nongshan Formation, and ends in the Guchengcun Formation. We measured and described this section, using a Jacob staff and an Abney level. The GPS location and stratigraphic level were recorded for each sample site as well as for any fossil localities that could be correlated directly with the line of section. There is an extensive covered interval that lies between the top of the CGD section and the base of the DT05 section. We used trigonometric projection to estimate that this gap represents ~350 m of stratigraphic thickness.

Paleomagnetic samples were taken as oriented hand samples, to be cut into ~2.5-cm cubes, or were drilled as oriented 1-inch-diameter cores. Four to six samples were collected from each of the 99 sample sites (43 in the CGD section and 56 in the DT05 section). Average sample spacing (excluding the gap between sections) was 9.2 m. All analyses were conducted in the paleomagnetics laboratory at the University of New Hampshire with an HSM2 SQUID cryogenic magnetometer, a Molspin tumbling alternating-field demagnetizer, and an ASC Model TD48 SC thermal demagnetizer. Pilot samples were analyzed with a variety of demagnetization protocols. Stepwise thermal demagnetization (12–14 steps) up to 690°C was found to be most effective for these red beds, so that method was applied to the rest of the samples. Remanence components were determined by least squares analysis, and site statistics were determined with the methods of Fisher (1953). Virtual geomagnetic pole (VGP) positions were calculated for each site, and these were averaged to calculate a mean paleomagnetic pole for the entire study.

Pedogenic carbonate nodules were collected from freshly exposed rock surfaces throughout the CGD and DT05 sections. Nodules were polished flat on a lapidary wheel, washed, and then dried overnight. For large nodules, primary micritic carbonate (~100–200 μg) was drilled from the polished surface with a mounted dental drill under a binocular microscope. Samples too small to drill were crushed to fine powder with a mortar and pestle. Samples were analyzed with the Optima gas source mass spectrometer in the Stable Isotope Lab at the University of California, Santa Cruz, with an automated Isocarb device after reaction with 100% phosphoric acid at 90°C. Carbon and oxygen isotope values are reported in delta notation relative to the VPDB (Vienna PDB) standard. Analytical precision, based on the standard deviation for repeated analysis of the NBS 19 standard, was <0.06‰ for carbon and <0.12‰ for oxygen.

Results

Paleomagnetic samples exhibited very stable thermal demagnetization behavior with one or two components of magnetization (fig. 2). The characteristic remanent magnetization (ChRM) was typically isolated between 670° and 690°C, indicating a hematite carrier. The ChRM directions were used to calculate site statistics, which in turn were used to construct a magnetostratigraphy for the Late Cretaceous–Early Paleogene of the Nanxiong Basin. Paleomagnetic sites were coded according to their reliability, with alpha sites ($n = 81$) being those with three or more stable samples that are significantly clustered at $P = 0.05$ (Watson 1956) and beta sites ($n = 14$) being those that have only two samples that are nonetheless congruent with each other or those with well-clustered but clearly transitional directions (table A1, available in the online edition or from the *Journal of Geology* office). Beta sites are used here for purposes of magnetostratigraphy but are not included in the calculation of summary statistics because of their lower precision. Sites that did not meet either set of criteria ($n = 4$) were discarded.

Alpha sites exhibit antipodal directions, with an average declination/inclination of 11.5°/27.4° (95% cone of confidence around the mean $\alpha_{95} = 3.0°$) in tilt-adjusted coordinates when all reversed sites are inverted (fig. 3). This corresponds to a paleomagnetic pole with an average longitude/latitude of 250.2°/74.1° ($\alpha_{95} = 2.5°$), which is indistinguishable from the Paleocene pole for the South China Block of 274.9°/78.9° ($\alpha_{95} = 6.1°$; Clyde et al. 2008). The ChRM directions of the alpha sites pass the reversal test at the 95% confidence limit via the bootstrapping method (Tauxe 1998). When these paleomagnetic data are plotted against stratigraphic level, the CGD section has five well-defined polarity zones (A+, B−, C+, D−, E+; fig. 4), whereas the DT05 section is characterized by a single long reversed-polarity zone (F−; fig. 5).

Paleosol carbonate samples from the Nanxiong CGD and DT05 sections have $\delta^{13}C$ values that range from −5‰ to −13‰ and $\delta^{18}O$ values ranging from −3‰ to −10‰ (fig. 6; table A2, available in the online edition or from the *Journal of Geology* office), consistent with those expected for a Late Cretaceous to Early Paleogene C3 ecosystem (e.g., Koch et al. 2003). Two to four replicate samples

Figure 2. Representative vector endpoint diagrams of paleomagnetic samples analyzed from the Nanxiong Basin. Open (filled) symbols show vector endpoints in the vertical (horizontal) plane. All directions are shown in tectonically corrected coordinates.

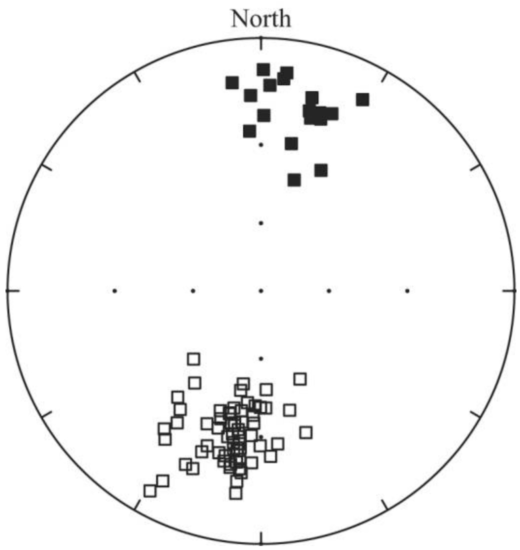

Figure 3. Equal-area projection of mean site directions for alpha sites from the Nanxiong Basin. Open (filled) symbols lie on the upper (lower) hemisphere of the projection. All directions are shown in tectonically corrected coordinates.

from each nodule were analyzed, and the average between-replicate difference was 0.23‰ in $\delta^{13}C$ and 0.31‰ in $\delta^{18}O$. In the CGD section, average $\delta^{13}C$ values range between −8‰ and −9‰ and show relatively little variability in the Cretaceous Pingling Formation but drop to between −9‰ and −12‰ and show much greater variability in the lower Shanghu Formation. Average $\delta^{18}O$ values show high variability in the Pingling Formation and increase by ~3‰ through the Shanghu Formation. The stratigraphically higher DT05 section show high variability in average $\delta^{13}C$ values, superimposed on an up-section increase of ~7‰, and variable but relatively stationary $\delta^{18}O$ values through the Nongshan and Guchengcun formations.

Discussion

Poorly documented radiometric ages reported from nearby locations constrain the correlation of our Nanxiong Basin magnetostratigraphy. Zhao et al. (1991) report two K-Ar ages (67.04 ± 2.34 and 67.7 ± 1.49 Ma) from the Yuanpu Formation, which underlies the Pingling Formation. Rigby et al. (1993) reported an age of 66.7 ± 0.30 Ma from $^{40}Ar/^{39}Ar$ analysis of three basalt flows ~1000 m below the top of the Nanxiong Group. These radiometric ages are consistent with abundant biostratigraphic information, indicating that the Pingling Formation is latest Cretaceous in age. This means that the normal- to reversed-polarity transition in the upper Pingling Formation at the base of our Nanxiong section (zone A+ to B−) must represent the Chron C30N to C29R reversal. Assignments of the remaining CGD polarity zones easily fall into place, assuming a relatively uniform sediment accumulation rate with zone C+ correlated with C29N, zone D− with C28R, and zone E+ with C28N (fig. 7 and Correlation 1 in fig. A1, available in the online edition or from the *Journal of Geology* office). A single well-defined reversed-polarity site within zone C+ is interpreted here to be either a spurious overprint or a cryptochron within Chron C29N, but it is conceivable that it represents Chron C28R, which would cause all other stratigraphically higher polarity-zone assignments to be advanced by one chron relative to our favored correlation (e.g., zone D− with C27R, zone E+ with C27N, etc.). This alternative correlation would require very rapid changes in sediment accumulation rates within the Shanghu Formation, for which we see no sedimentological evidence (fig. A1, Correlation 2). Correlation of polarity zone F− from the DT05 section is more complicated, but given its great thickness and the corresponding increase in carbon isotopic composition of paleosol carbonate, we correlate it with C26R, which is the longest reversed chron in the entire Cenozoic and also corresponds to a pattern of increasing carbon isotope values in other marine and continental settings (Zachos et al. 2001; Clyde et al. 2008). Other correlations for F− would require large changes in sediment accumulation rates in the DT05 section relative to the CGD section that are not supported by field observations and would be inconsistent with the sustained subsidence typical of extensional basins like this one (fig. A1, Correlation 3). Given our preferred correlation, these data establish the continuity of the Late Cretaceous to Paleocene section in the Nanxiong Basin and provide no support for the existence of a hiatus or unconformity representing >5 m.yr. at the K/Pg boundary, as previously suggested by Mateer and Chen (1992) and Russell et al. (1993).

K-Pg Boundary. The K-Pg boundary falls within the upper half of Chron C29R in all sections where it has been carefully constrained (e.g., Alvarez et al. 1977; Lerbekmo and Coulter 1984; Swisher et al. 1993; Dinarès-Turell et al. 2003; Hicks et al. 2003; Peppe et al. 2009). Preisinger et al. (1986) reviewed marine sections with the most precise magnetostratigraphies and found the K/Pg boundary ~70% up Chron C29R. The bottom and top of Chron C29R are well constrained in our new Nan-

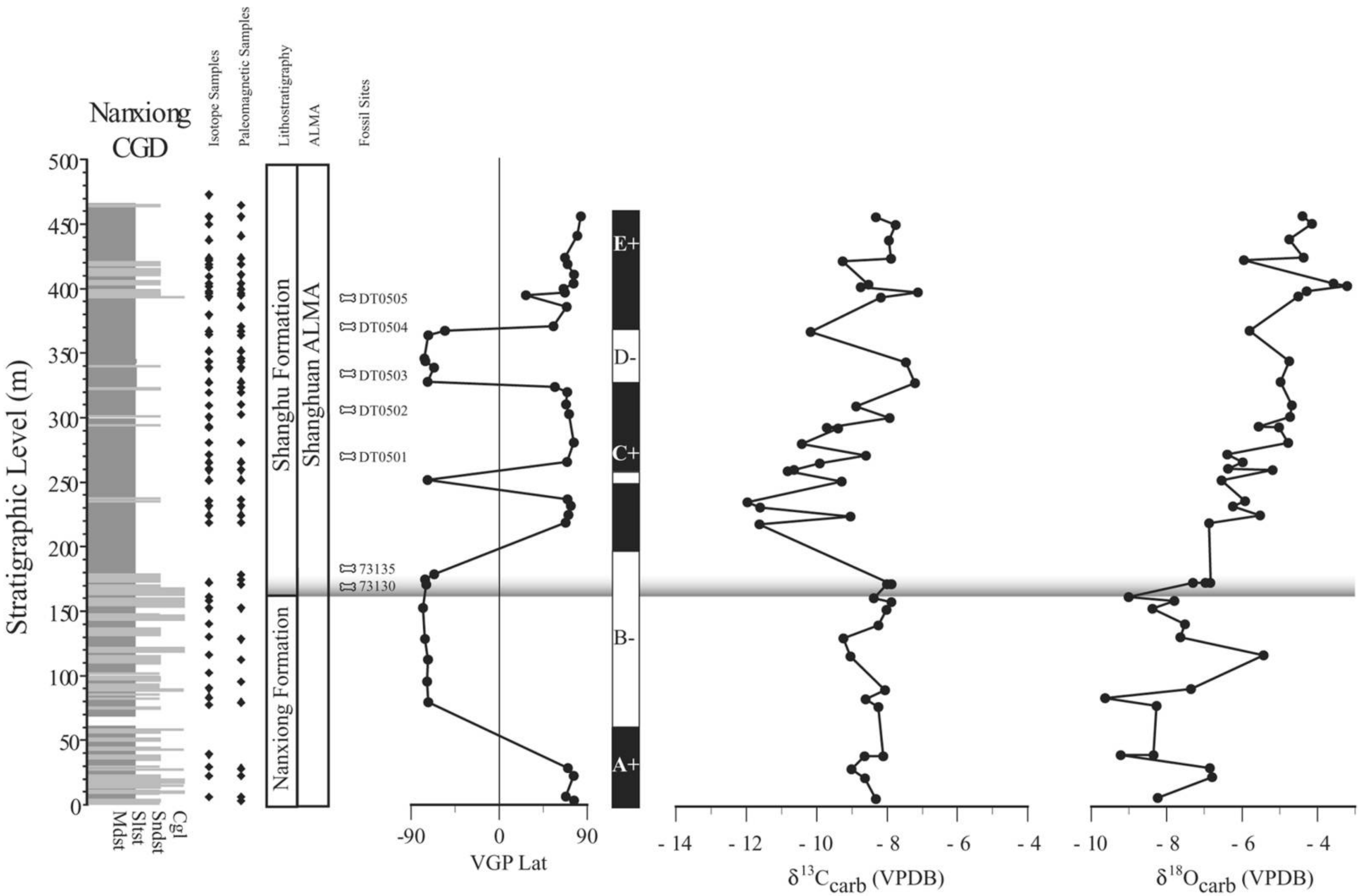

Figure 4. The CGD stratigraphic section from the Nanxiong Basin, showing (from left to right) the lithological log; the stratigraphic position of isotope, paleomagnetic, and fossil samples; magnetostratigraphic results; and stable-isotope results. Stratigraphic level according to Zhao et al. (1991) and Stets et al. (1996). ALMA = Asian Land Mammal Age. A color version of this figure is available in the online edition or from the *Journal of Geology* office.

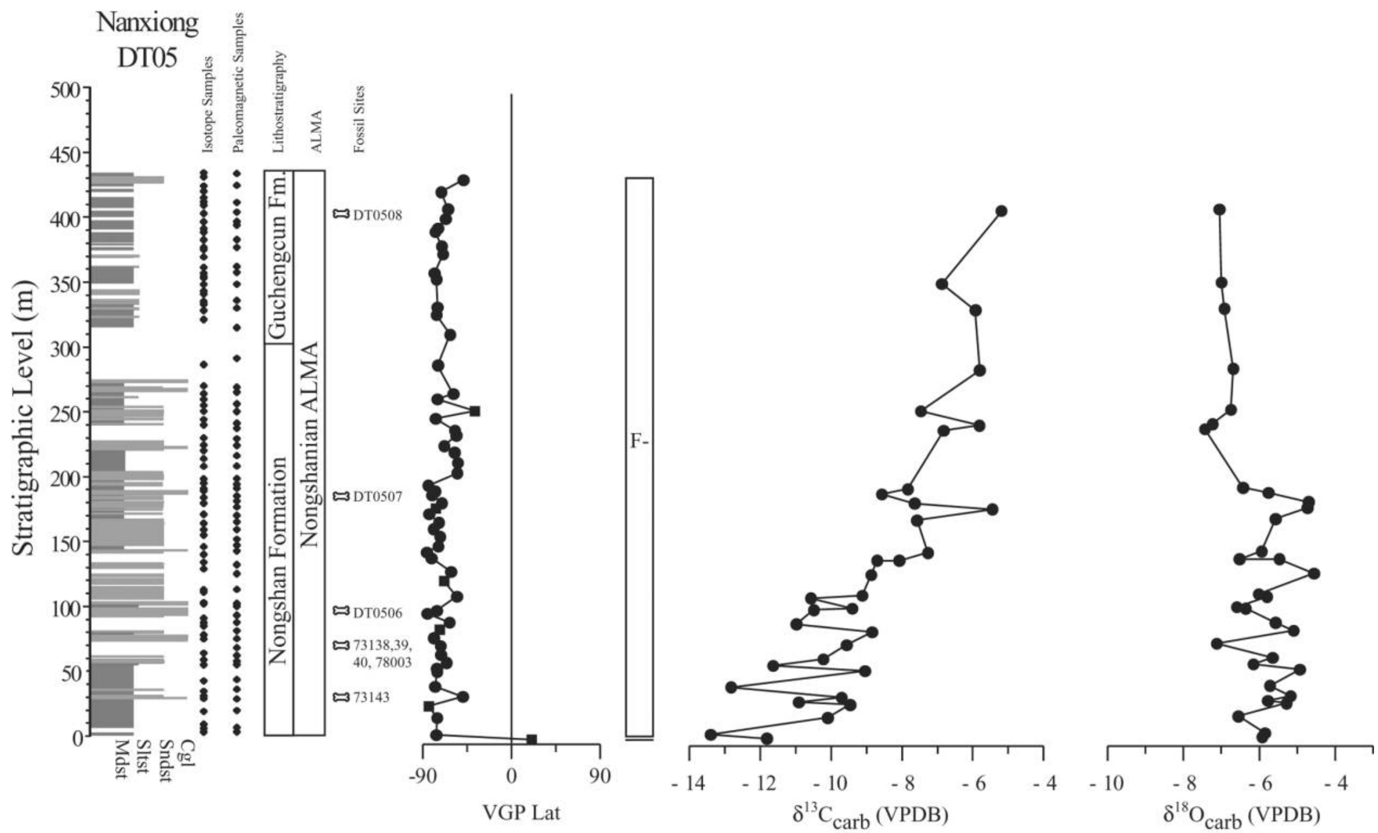

Figure 5. The DT05 stratigraphic section from the Nanxiong Basin, showing (from left to right) the lithological log; the stratigraphic position of isotope, paleomagnetic, and fossil samples; magnetostratigraphic results; and stable-isotope results. ALMA = Asian Land Mammal Age. A color version of this figure is available in the online edition or from the *Journal of Geology* office.

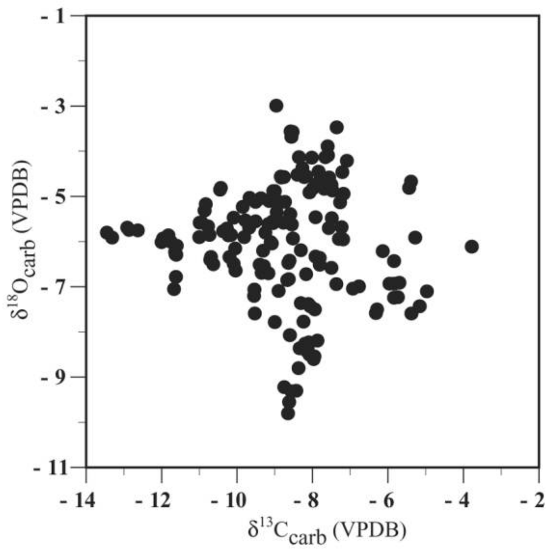

Figure 6. Bivariate plot of carbon and oxygen stable-isotope results from Nanxiong Basin, showing no correlation.

xiong magnetostratigraphy (polarity zone B−), allowing for evaluation of the competing placements of the K/Pg boundary in this basin. The Stets placement of the K/Pg boundary in the Nanxiong section lies only ~5% above the base of Chron C29R, whereas the Zhao placement of the K/Pg boundary lies ~74% above the base of Chron C29R. Clearly, the traditional Zhao K/Pg boundary placement correlates more closely with the globally recognized K/Pg boundary.

Aside from this new paleomagnetic evidence supporting the Zhao K/Pg boundary placement, there are other biotic, lithological, and isotopic changes at this level that may represent direct responses to the K/Pg impact event. This is important, given that the Nanxiong Basin is on the opposite side of Earth from the putative K/Pg impact site and that there is interest in understanding the spatial distribution of the impact's effects. Lithologically, the boundary is marked by an interval of unusual conglomeratic sandstones with noticeably distorted bedding. These sandstone beds also mark the transition from a coarser-grained, higher-energy depositional system that dominated during the Cretaceous to a finer-grained, lower-energy depositional system that dominated during the Paleogene. It is quite possible that the unusual lithologies at the boundary and the larger-scale depositional changes record the short- and long-term effects, respectively, of the K/Pg perturbation on the Nanxiong landscape (Fastovsky et al. 2008). Biotically, the clearest evidence of turnover comes at the boundary itself, where abundant evidence of dinosaurs, in the form of egg shells and egg shell fragments, disappears and Paleocene mammals first appear, all within the conglomeratic interval that marks the boundary. The lack of a major pollen turnover at the K/Pg boundary in the Nanxiong Basin is perplexing and needs more detailed attention. The turnover highlighted by Stets et al. (1996), however, is clearly lower than the K/Pg boundary and thus may represent Late Cretaceous climatic changes that preceded the boundary impact event. In general, the stratigraphic ranges and environmental preferences of Late Cretaceous to Early Paleogene pollen taxa in eastern Asia are poorly resolved, so patterns in their occurrence are difficult to interpret.

The carbon isotopic composition of paleosol carbonate shows a significant change near the K/Pg boundary, suggesting a major shift in carbon cycling at this time. Average $\delta^{13}C$ values decrease by >2‰ in the Early Paleocene and exhibit high-frequency variability that is not observed in the Cretaceous. A transient negative excursion in surface-water carbonate and a reduction of the surface- to deep-water $\delta^{13}C$ gradient in the oceans have been interpreted as representing the temporary collapse and recovery of shallow marine ecosystems (and the biological pump) in response to the impact event (D'Hondt et al. 1998; Coxall et al. 2006). The shift in surface-water isotopic composition, perhaps accompanied by release of ^{13}C-depleted carbon to the atmosphere by continental biomass burning, would have forced a global shift in the $\delta^{13}C$ values of Earth-surface carbon pools. Many other continental sections also exhibit a negative carbon isotope anomaly coincident with the K-Pg boundary (e.g., Arens and Jahren 2000; Beerling et al. 2001; Maruoka et al. 2007). In our record, as in these other continental records, $\delta^{13}C$ values return to Late Cretaceous levels after ~1 m.yr., indicating that the longer-term (~3-m.yr.) recovery of the biological pump was decoupled from the more rapid recovery of atmospheric $\delta^{13}C$ values. Both the pace of the recovery and the relatively large magnitude of the $\delta^{13}C$ change in the terrestrial records suggest that the K-Pg continental carbon cycle was affected by additional factors beyond the collapse of the biological pump, potentially including the global effects of widespread biomass burning and local changes in carbon cycling due to alteration of terrestrial ecosystems. Carbonate samples within the chaotically bedded K/Pg boundary interval from our Nanxiong section have $\delta^{13}C$ values similar to underlying Cretaceous values. This could represent a slight time

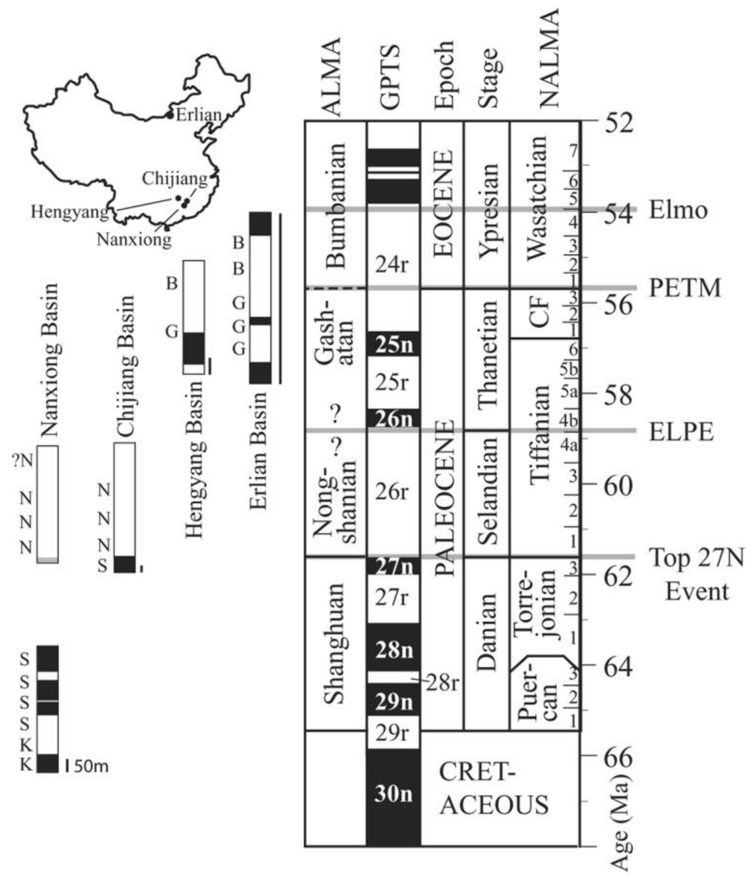

Figure 7. *Left*, Fence diagram of all Paleocene mammal-bearing continental sections in eastern Asia, with independent chronostratigraphic constraints and map showing locations of sites (Bowen et al. 2002, 2005; Ting et al. 2003; Clyde et al. 2008; this study). Scale bar represents 50 m of stratigraphic thickness in each section. The letters B, G, N, and S correspond to the Bumbanian, Gashatan, Nongshanian, and Shanghuan Asian Land Mammal Ages (ALMAs), respectively; K = Cretaceous. *Right*, Composite chronostratigraphy, showing inferred relationship between ALMA boundaries and North American Land Mammal Age (NALMA) boundaries. Shaded bars represent hyperthermal events (e.g., the Early-Late Paleocene Biotic event [ELPE], the Paleocene-Eocene Thermal Maximum [PETM], and Elmo) or other geochemical anomalies (e.g., the Top C27N event) observed in deep-sea records. Timescale after Gradstein et al. (2004; GPTS = Geomagnetic Polarity Time Scale).

lag between the immediate (e.g., depositional and faunal) effects of the impact event and the subsequent collapse of the carbon cycle or, more likely, the result of reworking in this depositionally chaotic interval.

Mammalian Biochronology and Dispersal. The Nanxiong Basin represents the type section for the first two Paleocene ALMAs of the Cenozoic, the Shanghuan and the Nongshanian. The correlation of these ALMAs with land mammal age frameworks on other continents and with the geological timescale has been uncertain because of the lack of precise, well-documented age constraints from sections where mammal fossils are found. Our paleomagnetic and isotopic data from the Nanxiong section provide new insight in this regard. Russell et al. (1993) argued that the Shanghuan correlates with the Middle Paleocene, which would correspond to the Tiffanian North American Land Mammal Age (NALMA). Our results clearly show that the Shanghuan ALMA is Early Paleocene in age (Danian) and corresponds to the Puercan NALMA and at least part of the Torrejonian NALMA. Recent results from the Chijiang Basin argue for the placement of the Shanghuan-Nongshanian ALMA boundary near the top of Chron C27N (Clyde et al. 2008). This correlation implies that the Shanghuan-Nongshanian ALMA boundary is synchronous with the Torrejonian-Tiffanian NALMA boundary and corresponds to geochemical changes observed at the top of Chron C27N in deep marine sections. Our results from the Nanxiong Basin are consistent with this interpretation, although the boundary itself lies in the covered interval between the top of the CGD section (Chron C28N) and the base of the DT05 section (Chron C26R). The entire DT05 section, including the Nongshan and Guchengcun formations, seems to be characterized by Nongshanian mammals and is interpreted here as correlating with Chron C26R. This means the Nongshanian ALMA correlates with at least the first half of the Tiffanian ALMA. The timing of the Nongshanian-Gashatan ALMA boundary has not been precisely constrained anywhere in Asia. However, the results reported here, in combination with those from the Erlian Basin of Inner Mongolia and the Hengyang Basin of Hunan Province, indicate that it must lie somewhere between the upper part of Chron C26R and Chron C25N (Bowen et al. 2002, 2005; Ting et al. 2003; fig. 7).

Conclusions

A new integrated paleomagnetic, isotopic, and biostratigraphic data set from the Nanxiong Basin of South China resolves previous uncertainty concerning the placement of the K/Pg boundary and constrains the timing of Asian Early Paleocene mammalian evolution. Traditional placement of the K/Pg boundary at the lithological contact between the Pingling and Shanghu formations lies within the upper half of Chron C29R, consistent with all other precisely constrained K/Pg boundaries in the world. This boundary also marks the highest occurrence of dinosaur fossils (eggshells) and the lowest occurrence of Paleocene mammals, indicating that the continental biotic response in Asia was synchronous with the impact despite its great distance from the putative impact site. Carbon isotopic records across the boundary are consistent with a major disruption to the carbon cycle and a relatively rapid recovery, compared to that in marine systems. These new data also constrain the timing of Early Paleocene mammalian recovery and turnover in the basin and support the placement of the Shanghuan-Nongshanian ALMA boundary near the top of Chron C27, coincident with similar biotic turnover in North America and geochemical changes in the deep sea.

ACKNOWLEDGMENTS

This research was funded by National Geographic Society grant 7329-02 and National Science Foundation grant EAR0540835. We thank S. Xie of the Institute of Vertebrate Paleontology and Paleoanthropology (IVPP), W. Zhou of the IVPP, and the county government of Nanxiong for their help with fieldwork. G. Messe, E. Crete, and K. Warren of University of New Hampshire helped with paleomagnetic measurements. Comments from D. E. Fastovsky were helpful during revision of the manuscript.

REFERENCES CITED

Alvarez, W.; Arthur, M. A.; Fischer, A. G.; Lowrie, W.; Napoleone, G.; Premoli Silva, I.; and Roggenthen, W. M. 1977. Upper Cretaceous–Paleocene magnetic stratigraphy at Gubbio, Italy V. Type section for the Late Cretaceous–Paleocene geomagnetic reversal time scale. Geol. Soc. Am. Bull. 88:383–389.

Arens, N. C., and Jahren, A. H. 2000. Carbon isotope excursion in atmospheric CO_2 at the Cretaceous-Tertiary boundary: evidence from terrestrial sediments. Palaios 15:314–322.

Beerling, D. J.; Lomax, B. H.; Upchurch, G. R. J.; Nichols, D. J.; Pillmore, C. L.; Handley, L. L.; and Scrimgeour, C. M. 2001. Evidence for the recovery of terrestrial ecosystems ahead of marine primary production following a biotic crisis at the Cretaceous-Tertiary boundary. J. Geol. Soc. Lond. 158:737–740.

Bowen, G. J.; Clyde, W. C.; Koch, P. L.; Ting, S.; Alroy, J.; Tsubamoto, T.; Wang, Y.; and Wang Y. 2002. Mammalian dispersal at the Paleocene/Eocene boundary. Science 295:2062–2065.

Bowen, G. J.; Koch, P. L.; Meng, J.; Ye, J.; and Ting, S. 2005. Age and correlation of fossiliferous Late Paleocene–Early Eocene strata of the Erlian Basin, Inner Mongolia, China. Am. Mus. Novit. 3474:1–26.

Buck, B. J.; Hanson, A. D.; Hengst, R. A.; and Shu-sheng, H. 2004. "Tertiary dinosaurs" in the Nanxiong Basin, southern China, are reworked from the Cretaceous. J. Geol. 112:111–118.

Clyde, W. C.; Tong, Y.; Snell, K. E.; Bowen, G. J.; Ting, S.; Koch, P. L.; Li, Q.; Wang, Y.; and Meng, J. 2008. An integrated stratigraphic record from the Paleocene of the Chijiang Basin, Jiangxi Province (China): implications for mammalian turnover and Asian block rotations. Earth Planet. Sci. Lett. 269:553–563.

Coxall, H. K.; D'Hondt, S.; and Zachos, J. C. 2006. Pelagic evolution and environmental recovery after the Cretaceous-Paleogene mass extinction. Geology 34:297–300.

D'Hondt, S.; Donaghay, P.; Zachos, J. C.; Luttenberg, D.; and Lindinger, M. 1998. Organic carbon fluxes and ecological recovery from the Cretaceous-Tertiary mass extinction. Science 282:276–279.

Dinarès-Turell, J.; Baceta, J. I.; Pujalte, V.; Orue-Etxebarria, X.; Bernaola, G.; and Lorito, S. 2003. Untangling the Palaeocene climatic rhythm: an astronomically calibrated Early Palaeocene magnetostratigraphy and biostratigraphy at Zumaia (Basque Basin, northern Spain). Earth Planet. Sci. Lett. 216:483–500.

Erben, H. K.; Ashraf, A. R.; Böhm, H.; Hahn, G.; Hambach, U.; Krumseik, K.; Stets, J.; Thein, J.; and Wurster, P. 1995. Die Kreide/Tertiär-Grenze im Nanxiong-Becken: Kontinentalfazies, Südostchina. Mainz, Steiner, 245 p.

Fastovsky, D. E.; Sheehan, P. M.; Isbell, J. L.; and Grandpre, R. 2008. Anomalous, temporary terrestrial sedimentary environments following Cretaceous-Tertiary ecosystem disruptions: North America, Asia, and Europe. Geol. Soc. Am. Abstr. Program 40:322.

Fisher, R. A. 1953. Dispersion on a sphere. Proc. R. Soc. A 217:295–305.

Gingerich, P. D. 2006. Environment and evolution through the Paleocene-Eocene thermal maximum. Trends Ecol. Evol. 21:246–253.

Gradstein, F. M.; Ogg, J. G.; and Smith, A. G. 2004. Geological time scale 2004. Cambridge, Cambridge University Press, 589 p.

Hansen, J. J.; Liu, Q.; Rasmussen, K. L.; and Gwozdz, R. 1994. The Cretaceous-Tertiary transition in South China. Hist. Biol. 7:251–263.

Hicks, J. F.; Johnson, K. R.; Obradovich, J. D.; Miggins, D. P.; and Tauxe, L. 2003. Magnetostratigraphy of upper Cretaceous (Maastrichtian) to lower Eocene strata of the Denver Basin, Colorado. Rocky Mt. Geol. 38: 1–27.

Koch, P. L.; Clyde, W. C.; Hepple, R. P.; Fogel, M. L.; Wing, S. L.; and Zachos, J. C. 2003. Carbon and oxygen isotope records from paleosols spanning the Paleocene-Eocene boundary, Bighorn Basin, Wyoming. *In* Wing, S. L.; Gingerich, P. D.; Schmitz, B.; and Thomas, E., eds. Causes and consequences of globally warm climates in the early Paleogene. Geol. Soc. Am. Spec. Pap. 369:49–64.

Lerbekmo, J. F., and Coulter, K. C. 1984. Magnetostratigraphic and biostratigraphic correlations of Late Cretaceous to Early Paleocene strata between Alberta and North Dakota. Mem. Can. Soc. Pet. Geol. 9:313–317.

Li, C. K., and Ting, S. Y. 1983. The Paleogene mammals of China. Bull. Carn. Mus. Nat. Hist. 21:1–93.

Maruoka, T.; Koeberl, C.; and Bohor, B. F. 2007. Carbon isotopic compositions of organic matter across continental Cretaceous-Tertiary (K-T) boundary sections: implications for paleoenvironment after the K-T impact event. Earth Planet. Sci. Lett. 253:226–238.

Mateer, N. J., and Chen, P. 1992. A review of the nonmarine Cretaceous-Tertiary transition in China. Cretac. Res. 13:81–90.

McKenna, M. C., and Bell, S. K. 1997. Classification of mammals above the species level. New York, Columbia University Press.

McKenna, M. C.; Chow, M.; Ting, S.; and Luo, Z. 1989. *Radinskya yupingae*, a perissodactyl-like mammal from the Late Paleocene of China. *In* Prothero, D. R., and Schoch, R. M., eds. The evolution of perissodactyls. Oxford Monographs on Geology and Geophysics, no. 15. New York, Oxford University Press, New York, p. 24–36.

Molina, E.; Alegret, L.; Arenillas, I.; Arz, J. A.; Gallala, N.; Hardenbol, J.; von Salis, K.; Steurbaut, E.; Vandenberghe, N.; and Zaghbib-Turki, D. 2006. The global boundary stratotype section and point for the base of the Danian Stage (Paleocene, Paleogene, "Tertiary," Cenozoic) at El Kef, Tunisia: original definition and revision. Episodes 29:263–273.

Peppe, D. J.; Evans, D. A. D.; and Smirnov, A. V. 2009. Magnetostratigraphy of the Ludlow Member of the Fort Union Formation (lower Paleocene) of the Williston Basin in North Dakota. Geol. Soc. Am. Bull. 121:65–79.

Preisinger, A.; Zobetz, E.; Gratz, A. J.; Lahodynsky, R.; Becke, M.; Mauritsch, H. J.; Eder, G.; et al. 1986. The Cretaceous/Tertiary boundary in the Gosau Basin, Austria. Nature 322:794–799.

Rigby, J. K., Jr.; Snee, L. W.; Unruh, D. M.; Harland, S. S.; Guan, J.; Li, F.; Rigby, J. K.; and Kowalis, B. J. 1993. $^{40}Ar/^{39}Ar$ and U-Pb dates for dinosaur extinction, Nanxiong Basin, Guangdong Province, People's Republic of China. Geol. Soc. Am. Abstr. Program 25: A296.

Russell, D. A.; Russell, D. F.; and Sweet, A. R. 1993. The end of the dinosaurian era in Nanxiong Basin. Vertebr. Palasiat. 31:139–145.

Stets, J.; Ashraf, A.; Erben, H. K.; Hahn, G.; Hambach, U.; Krumsiek, K.; Thein, J.; and Wurster, P. 1996. The Cretaceous-Tertiary boundary in the Nanxiong Basin (continental facies, southeast China). *In* MacLeod, N., and Keller, G., eds. Cretaceous-Tertiary mass extinctions: biotic and environmental changes. New York, Norton, p. 349–371.

Swisher, C. C. I.; Dingus, L.; and Butler, R. F. 1993. $^{40}Ar/^{39}Ar$ dating and magnetostratigraphic correlation of the terrestrial Cretaceous-Paleogene boundary and Puercan mammal age, Hell Creek-Tullock formations, eastern Montana. Can. J. Earth Sci. 30:1981–1996.

Tauxe, L. 1998. Paleomagnetic principles and practice. Dordrecht, Kluwer.

Taylor, L. H.; Jacobs, L. L.; and Downs, W. R. 2006. A review of the Cretaceous-Paleogene boundary in the Nanxiong Basin. *In* Lu, J. C.; Kobayashi, Y.; Huang, D.; and Lee, Y.-N., eds. Papers from the 2005 Heyuan International Dinosaur Symposium. Beijing, Geological Publishing House, p. 39–59.

Ting, S. 1998. Paleocene and Early Eocene land mammal ages of Asia. *In* Beard, K. C., and Dawson, M. R., eds. Dawn of the age of mammals in Asia. Bull. Carn. Mus. Nat. Hist. 34:124–147.

Ting, S.; Bowen, G. J.; Koch, P. L.; Clyde, W. C.; Wang, Y.; Wang, Y.; and McKenna, M. C. 2003. Biostratigraphic, chemostratigraphic, and magnetostratigraphic study across the Paleocene/Eocene boundary in the Hengyang Basin, Hunan, China. *In* Wing, S. L.; Gingerich, P. D.; Schmitz, B.; and Thomas, E., eds. Causes and consequences of globally warm climates in the early Paleogene. Geol. Soc. Am. Spec. Pap. 369: 521–535.

Tong, Y. 1979. A Late Paleocene primate from South China. Vertebr. Palasiat. 17:65–70.

Wang, X., and Zhai, R. 1995. *Carnilestes*, a primitive lipotyphlan (Insectivora: Mammalia) from the Early and Middle Paleocene, Nanxiong Basin, China. J. Vertebr. Paleontol. 15:131–145.

Wang, Y.; Hu, Y.; Chow, M.; and Li, C. 1998. Chinese Paleocene mammal faunas and their correlation. *In* Beard, K. C., and Dawson, M. R., eds. Dawn of the age of mammals in Asia. Bull. Carn. Mus. Nat. Hist. 34:89–123.

Watson, G. S. 1956. A test for randomness of directions. Mon. Not. R. Astron. Soc. Geol. Suppl. 7:160–161.

Zachos, J. C.; Pagani, M.; Sloan, L.; Thomas, E.; and Billups, K. 2001. Trends, rhythms, and aberrations in global climate 65 Ma to present. Science 292:686–693.

Zhao, A.; Te, J.; Li, H.; Zhao, Z.; and Tan, Z. 1991. Extinction of the dinosaurs across the Cretaceous-Tertiary boundary in Nanxiong Basin, Guangdong Province. Vertebr. Palasiat. 29:1–20.

Zhao, Z.; Mao, X.; Chai, Z.; Yang, G.; Kong, P.; Ebihara, M.; and Zhao, Z. 2002. A possible causal relationship between extinction of dinosaurs and K/T iridium enrichment in the Nanxiong Basin, south China: evidence from dinosaur eggshells. Palaeogeogr. Palaeoclimatol. Palaeoecol. 178:1–17.

Zhao, Z.; Wang, J.; Chen, S.; and Zhong, Y. 1993. Amino acid composition of dinosaur eggshells nearby the K/T boundary in Nanxiong Basin, Guangdong Province. Palaeogeogr. Palaeoclimatol. Palaeoecol. 104:213–218.